

Length-dependent thermal conductivity of single extended polymer chains

Jun Liu and Ronggui Yang*

Department of Mechanical Engineering, University of Colorado at Boulder, Boulder, Colorado 80309, USA

(Received 23 May 2012; revised manuscript received 15 August 2012; published 24 September 2012)

The low thermal conductivity of polymers will be one of the major roadblocks for the polymer-based microelectronics and macroelectronics due to the limited heat spreading capability. Despite that the thermal conductivity of bulk polymers is usually low, a single extended polymer chain could have very high thermal conductivity. In this paper we present atomistic simulation studies on the phonon transport in single extended polymer chains of various polymers as a function of polymer chain length. The thermal conductivity of single extended polymer chains can be 1–2 orders of magnitude higher than their bulk counterparts. The thermal conductivity of single extended polymer chains is a strong function of monomer type. For example, the thermal conductivity of the extended polymer chains with aromatic backbone can be up to 5 times as that of a polyethylene chain, while the thermal conductivity of the extended polymer chains with bond-strength or mass disorder can be only 1/25 as that of a polyethylene chain. We analyze the phonon transport mechanisms in single extended polymer chains of various polymers and find that the competition between ballistic phonon transport and diffusive phonon transport in a polymer chain leads to a diverging length-dependent thermal conductivity.

DOI: [10.1103/PhysRevB.86.104307](https://doi.org/10.1103/PhysRevB.86.104307)

PACS number(s): 63.22.-m, 65.40.-b, 66.70.Hk, 63.20.-e

I. INTRODUCTION

Polymer materials are generally regarded as thermal insulators because they have a universally low thermal conductivity of 0.1–1 W/mK at room temperature,¹ which is 2–3 orders of magnitude lower than their inorganic counterparts. One of the main reasons for the low thermal conductivity is that the polymer chains are randomly coiled in bulk polymers, as shown in Fig. 1(a), which effectively shortens the mean free path of heat-carrying phonons.² The low thermal conductivity of polymers will be one of the major roadblocks for polymer-based microelectronics and macroelectronics such as organic displays³ and organic solar cells⁴ due to the limited heat spreading capability.

Despite that the thermal conductivity of bulk polymers is usually low, a single extended polymer chain which has a well-aligned polymer segments, as illustrated in Fig. 1(b), could have very high thermal conductivity. For example, a recent molecular dynamics simulation shows that the thermal conductivity of a single polyethylene chain can be as high as 350 W/mK with a chain length larger than 100 nm.⁵ This has recently been confirmed by the measurement on polyethylene nanofibers.⁶ When a polyethylene gel is drawn to 400 times of its original length to obtain polyethylene nanofibers with diameters of 50–500 nm, the thermal conductivity is increased to about 104 W/mK (~300 times that of bulk polyethylene). Another recent discovery is that an individual micrometer-size spider silk fiber has an exceptionally high thermal conductivity up to 416 W/mK due to the highly oriented polymer chains in silk fibers.⁷

Both the chain length and monomer type of polymer chains could affect the thermal conductivity. For instance, reports show that the thermal conductivity of a single extended polyethylene chain is 50 times that of a single extended polydimethylsiloxane chain and thermal conductivity of both chains increases with increasing chain lengths.^{5,8} With the development of the various techniques to practically obtain samples with more aligned polymer chains, such as mechanical stretching⁹ and the recently developed molecular layer

deposition technique,¹⁰ general design guidance for tuning the thermal properties of these materials with extended polymer chains is in critical need. In this work we study the dependence on the monomer type and the chain length of the thermal conductivity and phonon transport mechanism of single extended polymer chains using molecular dynamics simulations. This study could provide guidance for the development of advanced polymer products with high thermal conductivity.

II. SIMULATION METHOD

The objective for this work is to explore the dependence of thermal conductivity of single extended polymer chains on monomer type and chain length instead of precisely calculating the thermal conductivity of polymers either in their amorphous or crystalline states. To eliminate other factors that strongly affect the thermal transport in polymer chains, such as random orientation of chains in amorphous state and interchain interactions in the fully chain-extended crystals, and to identify particularly the effect of chain monomer type and chain length, we have thus chosen single extended chains that free from random orientations and interchain interactions in this work.

A. Material model of single extended polymer chains

We investigated single extended polymer chains of eight different polymer monomers as shown in Table I to study the effect of the monomer types on the phonon transport. Poly(*p*-phenylene) and polybenzimid are the two representative polymer chains with aromatic backbone. In aromatic backbone structures, the monomer usually contains planar cyclic rings or ringlike structures. Compared to polyethylene, polyacetylene has double bonds in the aliphatic chains. We also studied the effect of chain disorder on phonon transport in single extended polymer chains, which includes bond-strength disorder, mass disorder, and orientation disorder. We note that these “chain disorders” termed in this paper are only for the convenient comparisons among polymer chains of different monomer types and are not the same as the disorders

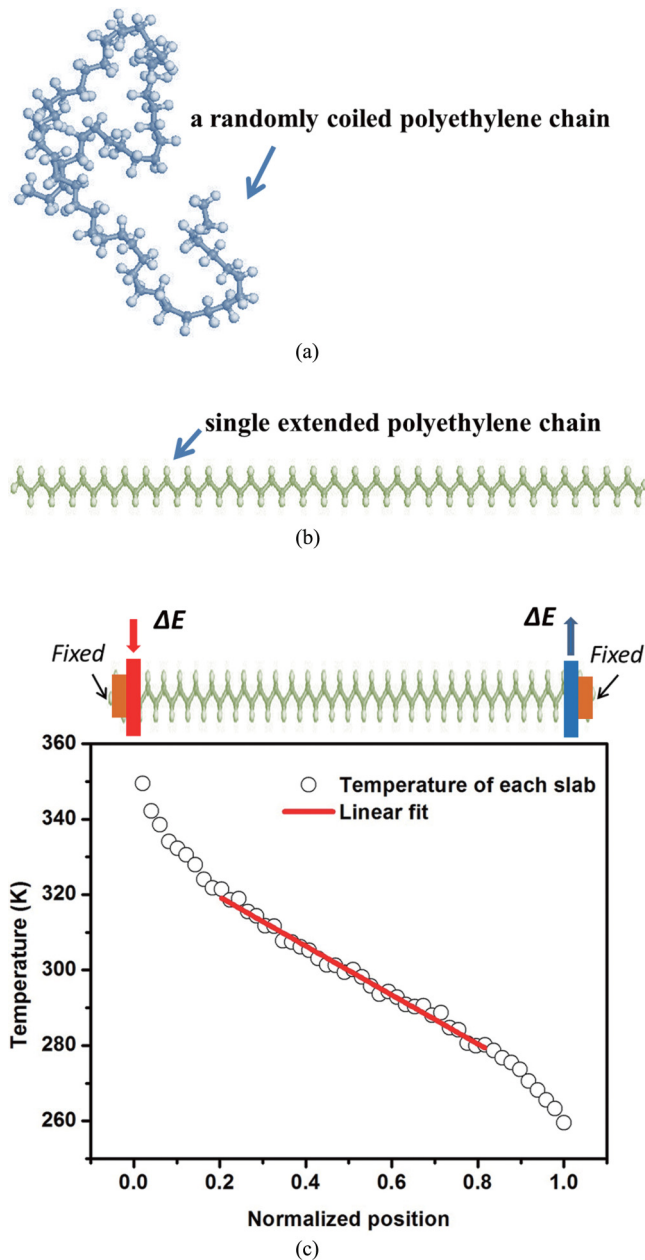


FIG. 1. (Color online) (a) Schematic drawing of a randomly coiled polyethylene chain. The random orientation of the chain segments is one of the main reasons for the low thermal conductivity of bulk polymers. (b) Schematic drawing of a single extended polyethylene chain. A single extended polymer chain with well-aligned polymer segments might have high thermal conductivity. (c) Upper panel: a typical NEMD simulation system for the thermal conductivity of a single extended polymer chain. The simulation system was divided into several slabs (20 to 50 slabs, depending on the total length), each with a thickness δ . At each end, the atoms in one slab were fixed to act as a heat-insulating wall. A small amount of heat ΔE (~ 10 J/mol) was added into the slab adjacent to the fixed slab (hot region) at each time step; the same amount of heat was removed from the slab adjacent to the fixed slab at the other end (cold region). Lower panel: a typical temperature profile in the simulation domain. The linear temperature region was fitted using the least-square method to obtain the temperature gradient dT/dx for the calculation of the effective thermal conductivity using the Fourier's law of heat conduction.

(e.g. weak disorder such as defects and dislocations, and strong disorder such as in liquid, amorphous solids, and composites) commonly defined in solid state physics. There are alternating single carbon-carbon bonds and double carbon-carbon bonds in polybutadiene. When the covalent bonds with different strengths are mixed together in a chain, we term it as bond-strength disorder in this paper. The mass disorder we termed here is generated by the incorporation of other elements or functional groups with different masses into an otherwise aliphatic or aromatic pristine chain. For example, poly(oxyethylene) and poly(ethylene oxide) can be viewed as incorporating oxygen atoms into a polyethylene chain. Similarly, incorporating oxygen atoms into a poly(*p*-phenylene) chain leads to a poly(phenylene ether) chain. Orientation disorder, which can be observed in poly(*p*-phenylene) and poly(phenylene ether), is the misalignment of the orientation of aromatic rings compared to the well-aligned aromatic rings in the chain.

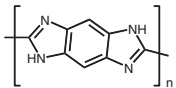
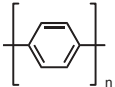
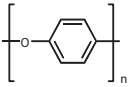
In our polymer model, each atom is treated as a single site and assigned a corresponding mass. The interactions between atoms are described by the polymer consistent force field (PCFF).¹¹ The force cutoff distance was 10 Å. The software package Material Studio^{®12} is used to build the initial configuration of the single extended polymer chains by connecting together multiple segments of the polymer monomers. For instance, after energy optimization of the ethylene monomer ($-\text{CH}_2-\text{CH}_2-$) by adjusting the atomic coordinates iteratively to reach the minimum energy, a single polyethylene chain is obtained by replicating the monomer in the chain backbone direction, as shown in Fig. 1(b). The repeating units of polymer chains are called segments in this paper.

B. NEMD simulation for thermal conductivity

The thermal conductivity of single extended polymer chains was calculated using the nonequilibrium molecular dynamics (NEMD) simulation of the LAMMPS simulation package.^{13–16} A schematic representation of the simulation system used to compute the thermal conductivity is shown in the upper panel of Fig. 1(c). The simulation system was divided into several slabs (20 to 50 slabs, depending on the total length), each with a thickness δ . To keep the extended-chain state, which is an entropically unfavorable state, the atoms in one slab at each end were fixed to act as a heat-insulating wall. The force at the chain ends eventually evolves into the tensile stress on the polymer chains. The tensile stress in the single extended polymer chains might have some effects on the thermal conductivity values, which is discussed in Sec. III A. To choose a proper time step for the simulations, we have tested the time steps of 1 and 0.5 fs in our simulations. Using both time steps, the temperature and energy of the system is stable and the difference of the calculated values of thermal conductivity is within 5%. The results presented in this work are calculated using 1 fs as the time step.

Before calculating the thermal conductivity, all the samples were relaxed to release the thermal stress by employing a constant-*NVT* (constant number of particles, volume, and temperature) ensemble at a prescribed temperature (300 K) and then a constant-*NVE* (constant number of particles, volume,

TABLE I. Eight different types of polymers are investigated in this work. The effective cross-sectional area A of a single extended polymer chain is calculated by dividing the effective volume V_s of a polymer chain with its length L . Here we assume the effective volume of a single extended polymer chain V_s equals the volume of a polymer chain in the amorphous state with fully relaxed and coiled chain orientation V_a . The exponent β is the index when the length-dependent diverging thermal conductivity κ is fitted with the chain length L using $\kappa \sim L^\beta$, as discussed in Sec. III C.

Name	Chemical structure	Effective density (g/cm ³)	Effective cross-sectional area A (Å ²)	β
Polyethylene	$-\text{[CH}_2\text{-CH}_2\text{]}_n\text{-}$	0.74	24.66	0.438 ± 0.009
Polyacetylene	$-\text{[CH}=\text{CH]}_n\text{-}$	0.88	19.53	0.689 ± 0.019
Polybutadiene	$-\text{[CH}_2\text{-CH}=\text{CH-CH}_2\text{]}_n\text{-}$	0.78	19.34	0.417 ± 0.007
Polybenzimid		1.27	25.28	0.881 ± 0.046
Poly(<i>p</i> -phenylene)		1.17	26.65	N/A
Poly(phenylene ether)		1.10	30.55	N/A
Poly(methylene oxide)	$-\text{[CH}_2\text{-O]}_n\text{-}$	1.20	17.37	0.564 ± 0.067
Poly(ethylene oxide)	$-\text{[CH}_2\text{-CH}_2\text{-O]}_n\text{-}$	1.02	28.08	0.287 ± 0.023

and energy) ensemble. The thermostat for the constant- NVT and constant- NVE ensembles is Nose-Hoover.¹⁷ Typically it takes about 1–2.5 ns to relax the system so that stable values of temperature, pressure, and energy of the system can be reached. To obtain thermal conductivity, a small amount of heat ΔE (~ 10 J/mol) was added into the slab adjacent to the fixed slab (hot region) at each time step to create a heat flux along the x direction (the chain backbone direction) of the simulation system. The same amount of heat was removed from the slab adjacent to the fixed slab at the other end (cold region). The heat flux J along the x direction is then calculated as $J = \Delta E / A \Delta t$, where A is the effective cross-sectional area and Δt is the time step.

The effective cross-sectional area A of a single extended polymer chain is calculated by dividing the effective volume V_s of a polymer chain with its length L . Here we assume the effective volume of a single extended polymer chain V_s equals the volume of a polymer chain in the amorphous state with fully relaxed and coiled chain orientation V_a .⁸ We have calculated the effective cross-sectional area of the polymers using the densities of fully amorphous state rather than taking the cross-sectional area of perfect crystals based on the following reasons: (1) Not all the crystallography data for the perfect crystals of the polymers we studied can be found in literature. To make a reasonable comparison among eight types of polymers studied, a computationally consistent way is of great need. (2) Physically we are not computing the thermal conductivity of perfect polymer crystals. There are strong interchain interactions in perfect polymer crystals, which significantly affect the thermal transport in the crystal. We tend to believe that the cross-sectional area of a single chain should be closer to that in their amorphous state, where the chains has much weaker interactions. This methodology is similar to the calculation of carbon nanotubes, where a cross-sectional area corresponding to annular shell of width of 3.4 Å is used, the distance between the graphene planes in

graphite.¹⁸ We thus define the cross-sectional area using the volume of the amorphous polymers. Overall, the difference in these two definitions would be only a few percent, not significant enough to overshadow the conclusion of this work. Table I lists the effective density and the cross-sectional area for all the polymers studied. For instance, the simulation results in a density of 0.76 g/cm³ for ten 50-Å-long amorphous polyethylene chains at 300 K and 1 atm. The simulated density is lower than the measured density (0.9 g/cm³) of semicrystalline polyethylene samples because pure amorphous polymer materials are difficult to prepare in experiment,^{1,19} but very close to the density 0.79 g/cm³ obtained from quenching the polymer melt samples.¹⁹ Such a density 0.76 g/cm³ yields an effective cross-sectional area of 24.66 Å² for a single polyethylene chain. As a result, the effective cross-sectional area is larger than that of a polyethylene crystal where much stronger interchain interaction exists.

After the system reaches steady state, which typically takes 0.5–1 ns, the effective temperature of each slab was averaged over the following 2 ns. The lower panel of Fig. 1(c) shows a typical temperature profile. We then fit the linear temperature region using the least-square method to obtain the temperature gradient dT/dx so that the thermal conductivity κ can be calculated by $\kappa = J / (dT/dx)$, according to the Fourier's law of heat conduction. To reduce the statistical errors in the calculated thermal conductivity, the effective temperature of each slab was separately averaged over four consecutive 0.5 ns simulation times. Moreover, the thermal conductivity values were averaged over at least three simulations with different heat fluxes. The error bars shown in Fig. 2, around 5%, represent the percentage deviation of the averaged thermal conductivity from the thermal conductivities calculated from different simulation times and heat fluxes. The error bars are not plotted explicitly when they are small compared with the plot scales.

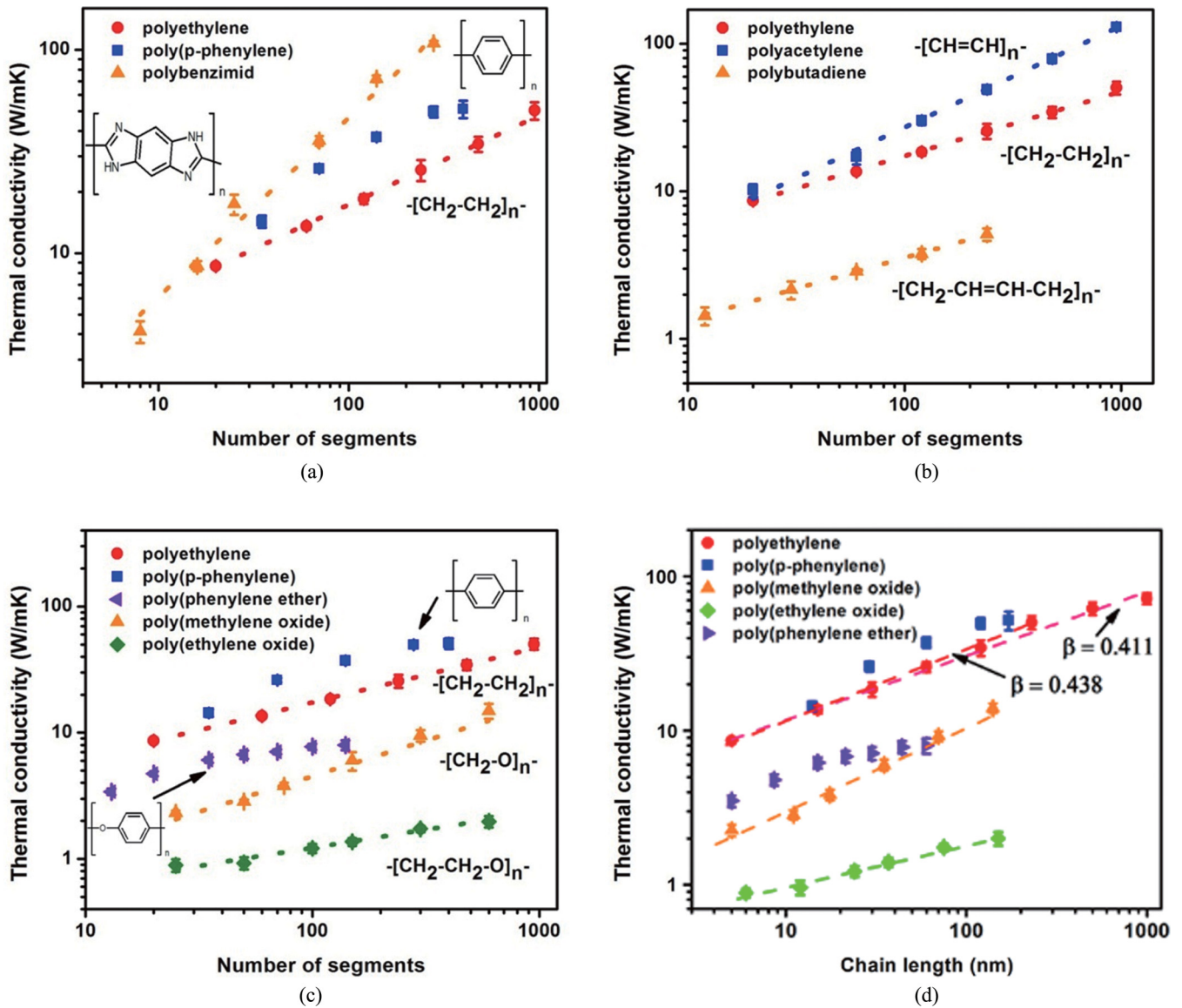


FIG. 2. (Color online) The thermal conductivity of single extended polymer chains of various polymers as a function of the number of segments: (a) effect of aromatic backbone; (b) effect of double bonds and bond-strength disorder compared to polyethylene; (c) effect of bond-strength disorder/mass disorder by incorporation of oxygen atoms in polyethylene; and (d) the thermal conductivity of single extended polymer chains of five polymers as a function of chain length.

III. RESULTS AND DISCUSSIONS

The molecular dynamics simulation results of the thermal conductivity of single extended polymer chains of various polymers as a function of the number of segments are presented in Sec. III A. The phonon transport mechanisms in these single extended polymer chains are presented in Sec. III B to explain the difference observed. Finally, the length-dependent thermal conductivity is analyzed in Sec. III C.

A. The effect of polymer types on the thermal conductivity

Figure 2 shows the thermal conductivity of single extended polymer chains of various polymers as a function of the number of segments, that is, the length of polymer chains. In general, the thermal conductivity of single extended polymer chains is 1–2 orders of magnitude higher than that of their bulk

counterparts,¹ 0.1–1 W/mK. When the number of segments (or the chain length) increases, the thermal conductivity of all types of simulated polymer chains increases. We note here that thermal conductivity of polymer chains with different monomer types is compared under the same number of segments.

Figure 2(a) shows that the thermal conductivity of the chains with aromatic-backbone structures is higher than that of aliphatic-backbone structures by comparing the thermal conductivity of poly(*p*-phenylene) and polybenzimid with that of polyethylene when the number of segments is larger than 20. The thermal conductivity of polybenzimid can be 4 times higher than that of polyethylene when the number of segments is 200. In the aromatic-backbone structure, carbon atoms form a planar ring by the conjugated π bonds. The sp^2 hybridization in aromatic-backbone structure is similar as that

in CNT and graphene, which makes this structure very stiff. Thermal conductivity usually increases with the increasing stiffness of the backbone as discussed in Ref. 8. Figure 2(b) shows that the thermal conductivity of polyacetylene is higher than that of polyethylene due to the stronger double bonds in polyacetylene. The bond strength of a double carbon-carbon bond is 1.82 times stronger than that of a single carbon-carbon bond.¹¹ The thermal conductivity of single extended polymer chains with double carbon-carbon bonds is up to 2.6 times that of a polyethylene chain. Interestingly, the thermal conductivity of polybutadiene is much lower than that of polyacetylene and polyethylene due to the bond-strength disorder, where there are mixing single and double carbon-carbon bonds in polybutadiene. Figure 2(c) shows that the thermal conductivity of poly(methylene oxide) is lower than that of polyethylene due to the mass disorder in the chain, where the oxygen atoms are incorporated in poly(methylene oxide) compared to polyethylene. The thermal conductivity of poly(ethylene oxide) is much lower than that of both polyethylene and poly(methylene oxide) due to both the bond-strength disorder and mass disorder presented in the chain compared to polyethylene. For instance, the thermal conductivity of poly(ethylene oxide) is only 1/25 as that of polyethylene when the number of segments is 600 or larger. Similarly, the thermal conductivity of poly(phenylene ether) is lower than that of poly(*p*-phenylene) due to the mass disorder in the chain compared to poly(*p*-phenylene). All the atoms or functional groups incorporated into the aliphatic/aromatic pristine chains can be viewed as mass disorder. Generally these mass disorders in the chain create localized vibrational modes, which impede the energy transport by delocalized, long-wavelength phonon modes and significantly reduce the thermal conductivity as that in alloys.²⁰ Similarly, Figure 2(d) shows the dependence of the thermal conductivity of single extended polymer chains of the five polymers as a function of chain length. Similar trends are seen as those observed in Fig. 2(c).

Indeed, a force must be applied at both ends of the chain to keep the chain in the extended configurations. All the motions of the monomers, including vibrational, translational, and torsional movement, are still allowed in the simulations. However, the motions of the monomers might become restricted depending on the force applied. The force applied at the chain ends eventually evolves into the tensile stress on the polymer chains. The tensile stress in the single extended polymer chains might have some effects on the thermal conductivity values compared to that in the coiled state of the polymer chains in bulk counterpart, as we showed in our previous paper.²¹ We have calculated how large of an effect that the tensile stress might have on the thermal conductivity in single extended polymer chains. Deformation simulation was performed on all the extended polymer chains studied. We found that the poly(*p*-phenylene) chain is the stiffest amongst all the polymer chains. When the polyethylene chain is stretched to have the same tensile stress as in the poly(*p*-phenylene) chain with the same number of segments, the increase of the thermal conductivity of polyethylene chain is less than 18%. The effect of the tensile stress on the thermal conductivity of polymer chains is a small factor compared to the effects of the monomer type and the chain length, thus the stress effect of extended polymer chains does not change the conclusions in this paper.

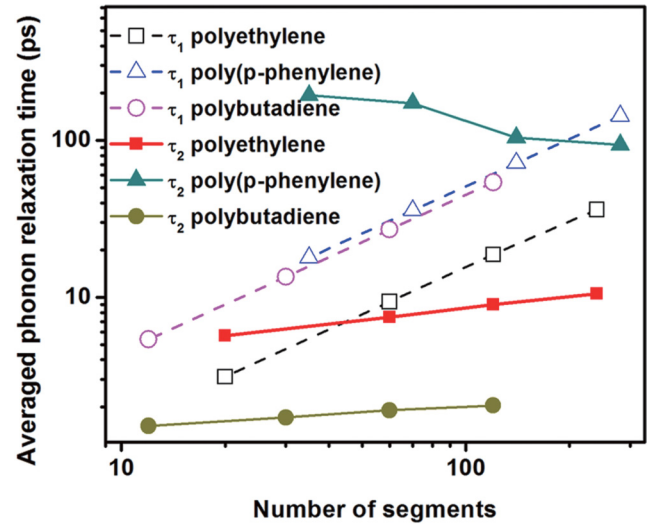


FIG. 3. (Color online) The averaged phonon boundary relaxation time τ_1 and the averaged intrinsic phonon relaxation time τ_2 of polyethylene, poly(*p*-phenylene), and polybutadiene chains as a function of the number of segments.

B. Phonon transport in single extended chains

In this section we calculate the averaged phonon relaxation time and analyze the dominant phonon scattering mechanisms in single extended polymer chains of different chain lengths. The averaged phonon relaxation time $\bar{\tau}$ can be calculated using the kinetic theory $\bar{\tau} = 3\kappa/C\bar{v}^2$, where κ is the thermal conductivity of an extended polymer chain, C is the volumetric heat capacity, and \bar{v} is the averaged phonon group velocity.²² We calculated the volumetric heat capacity C of different extended polymer chains using equilibrium molecular dynamics simulation. The *NVT* ensemble was applied for 2 ns to calculate the fluctuations in energy and temperature. The heat capacity is calculated by $C = (\langle E^2 \rangle - \langle E \rangle^2)/Vk_B\langle T \rangle^2$, where k_B is the Boltzmann constant, E , V , and T are the total energy, volume, and temperature of the simulated system, and $\langle \rangle$ represents the ensemble average.²³ The averaged phonon group velocity \bar{v} is calculated from the phonon dispersion curves of the single extended polymer chains, which is obtained by the standard lattice dynamics calculations using the GULP software package.²⁴ The phonon group velocity $v(\omega, p)$ at vibrational frequency ω and branch p is calculated as $v(\omega, p) = (\partial\omega/\partial q)_p$, where q is the wave number, with the phonon dispersion curve obtained. The averaged phonon group velocity \bar{v} is the arithmetic average over all the phonon dispersion branches and vibrational frequencies.

Using the Matthiessen rule, the averaged phonon relaxation time $\bar{\tau}$ can be written as

$$\frac{1}{\bar{\tau}} = \frac{1}{\tau_1} + \frac{1}{\tau_2}, \quad (1)$$

where τ_1 and τ_2 are the relaxation time of phonon-boundary scattering and intrinsic phonon relaxation time, respectively. By assuming τ_1 is L/\bar{v} , where L is the length between the two thermal reservoirs (hot region and cold region), τ_2 can then be calculated from Eq. (1). Figure 3 shows the relaxation time τ_1 of phonon-boundary scattering and intrinsic phonon relaxation time τ_2 of polyethylene, poly(*p*-phenylene),

and polybutadiene chains as a function of the number of segments. First, we analyze the dominant phonon transport mechanism in the single extended chains of different chain lengths. Phonon-boundary scattering dominates the phonon scattering mechanisms in a short polyethylene chain (number of segments $N < 60$). For example, the phonon boundary relaxation time τ_1 is 3.13 ps, whereas the intrinsic phonon relaxation time τ_2 is 5.69 ps in a 20-segment polyethylene chain. The thermal conductivity of short polyethylene chains are limited by the phonon-boundary scattering due to the limited length of the chain. Intrinsic phonon scattering dominates in a long polyethylene chain ($N > 200$). For example, the phonon boundary relaxation time τ_1 is 36.25 ps, while the intrinsic phonon relaxation time τ_2 is 10.54 ps in a 240-segment polyethylene chain. The dominant phonon transport mechanism in the poly(*p*-phenylene) chain is similar as that in the polyethylene chain. Phonon boundary scattering dominates the phonon scattering mechanisms in a short chain ($N < 100$) while intrinsic phonon scattering dominates in a long polymer chain ($N > 200$). If the polymer chain has any kind of “disorder,” such as bond-strength disorder in polybutadiene compared to polyethylene, the intrinsic phonon scattering has a dominant effect in phonon transport, as we can see that τ_2 is always shorter than τ_1 . Then we compare the phonon boundary relaxation time τ_1 among polyethylene, poly(*p*-phenylene), and polybutadiene chains. The phonon boundary relaxation time τ_1 of both poly(*p*-phenylene) and polybutadiene is larger than that of polyethylene. This result is due to the fact that the averaged phonon group velocity of poly(*p*-phenylene) is about half that of polyethylene due to the aromatic backbone. Similarly, the averaged phonon group velocity of polybutadiene is about 60% that of polyethylene due to the bond-strength disorder in polybutadiene compared to polyethylene. Last, we compare the intrinsic phonon relaxation time τ_2 among polyethylene, poly(*p*-phenylene), and polybutadiene chains. The intrinsic phonon relaxation time τ_2 of poly(*p*-phenylene) is much longer than that of polyethylene due to the aromatic backbone. The intrinsic phonon relaxation time τ_2 of polybutadiene is shorter than that of polyethylene due to the bond-strength disorder.

C. Length-dependent thermal conductivity

Figure 2(c) shows a very different length-dependent thermal conductivity of poly(*p*-phenylene) and poly(phenylene ether) than that of others, which converges when the number of segments increases. Such a convergent thermal conductivity indicates that the intrinsic phonon relaxation time decreases rapidly with increasing chain length, as can be seen in Fig. 3 for the poly(*p*-phenylene) chain. This occurs because the planar aromatic rings in the single extended chains of poly(*p*-phenylene) and poly(phenylene ether) can rotate around an imaginary axis formed by the two atoms connecting the adjacent functional groups. To understand how these rotations lead to orientation disorder in a chain and the differences between aliphatic chains and aromatic chains, we define the orientational parameter P_{2b} due to the backbone alignment as $P_{2b} = 1.5\langle(\mathbf{e}_1 \cdot \mathbf{e}_2)^2\rangle - 0.5$, where \mathbf{e}_1 and \mathbf{e}_2 are the backbone vector and $\langle \rangle$ represents the ensemble average, which is similar to the commonly used definition in an aliphatic chain.²¹

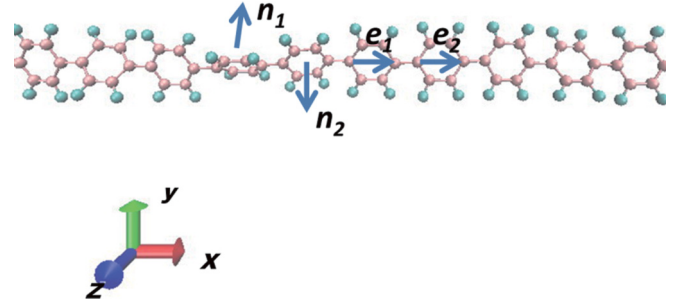


FIG. 4. (Color online) Schematic drawing shows the normal vector of planar aromatic rings \mathbf{n}_1 and \mathbf{n}_2 and the backbone vector \mathbf{e}_1 and \mathbf{e}_2 in the aromatic backbone structure.

Similarly, we define the orientational parameter P_{2rot} due to the planar aromatic ring rotation in the chain as $P_{2rot} = 1.5\langle(\mathbf{n}_1 \cdot \mathbf{n}_2)^2\rangle - 0.5$, where \mathbf{n}_1 and \mathbf{n}_2 are the normal vector of the planar aromatic rings. A schematic example is shown in Fig. 4 for the definition of the normal vector of planar aromatic rings \mathbf{n}_1 and \mathbf{n}_2 and the backbone vector \mathbf{e}_1 and \mathbf{e}_2 in the aromatic backbone structure. Table II shows the orientational parameters P_{2b} and P_{2rot} in poly(*p*-phenylene) and poly(phenylene ether) with two different chain lengths. The orientational parameters due to the backbone alignment P_{2b} for 16-segment and 400-segment poly(*p*-phenylene) are close to 1, which shows that the chain is still in the extended state during the simulation, the same as in the case of aliphatic chain. However, the orientational parameters due to the planar aromatic ring rotation P_{2rot} are 0.61 and 0.27 for 16-segment and 400-segment chains, respectively, which shows that the rotation misaligns the planar aromatic rings, creating the orientation disorders in the chain for phonon transport. P_{2rot} in a 16-segment chain is larger than that in a 400-segment chain, which indicates that more orientation disorders are generated in a relatively longer chain. The situation is similar in poly(phenylene ether), where the rotation of aromatic rings in the chain induces changes in chain orientation. Such increase of orientation disorders with the increasing chain length of planar aromatic rings explains well the converging length-dependent thermal conductivity in the single extended chains of poly(*p*-phenylene) and poly(phenylene ether).

Other than poly(*p*-phenylene) and poly(phenylene ether), most of the single extended polymer chains studied in Table I have a diverging length-dependent thermal conductivity. Similar diverging thermal conductivity behavior has been discussed in a number of low-dimensional materials such as harmonic lattice model,²⁵ 1D nonlinear lattice model,²⁶ Si

TABLE II. The orientational parameters due to the backbone alignment P_{2b} and the orientational parameters due to the planar aromatic ring rotation in the chain P_{2rot} in poly(*p*-phenylene) and poly(phenylene ether) chains with two different chain lengths.

	Poly(<i>p</i> -phenylene)		Poly(phenylene ether)	
	16 segments	400 segments	16 segments	400 segments
P_{2b}	0.98	0.97	0.49	0.45
P_{2rot}	0.61	0.27	0.16	0.09

nanowire,²⁷ CNT,²⁸ and more recently a single polyethylene chain.⁵ Similar to Li *et al.*,²⁹ we can fit the diverging thermal conductivity κ with the chain length L using $\kappa \sim L^\beta$ for these six types of polymer chains in Fig. 2. There are two regimes of phonon transport mechanisms in single extended polymer chains⁸: (1) Phonon propagates ballistically across the polymer chain before reaching the reservoir if the intrinsic phonon relaxation time is much larger than the relaxation time of phonon-boundary scattering; Such phonon-boundary scattering dominated transport is often called ballistic transport. (2) Phonon experiences numerous scattering event if the intrinsic phonon relaxation time is short, which is often called diffusive transport.³⁰ According to Li *et al.*,²⁹ β indicates the competition between diffusive and ballistic phonon transport, where diffusive phonon transport leads to $\beta = 0$ and ballistic phonon transport leads to $\beta = 1$. The weaker the phonon scattering, the closer is the β value to 1. Table I compares the exponent β for polymer chains with different monomer types. Polyacetylene has a higher β value than polyethylene due to the much weaker intrinsic phonon scattering mechanism in polyacetylene than that in polyethylene. Polybutadiene and poly(ethylene oxide) have a lower β value than polyethylene, and poly(phenylene ether) has a lower β value than poly(*p*-phenylene), which is due to the increased intrinsic phonon scattering in a chain with bond-strength/mass disorder compared to that in an otherwise aliphatic/aromatic pristine chain. However, poly(methylene oxide) chain does not seem to obey this rule. The β value of poly(methylene oxide) is even higher than that of polyethylene. Very likely, even though the mass disorder in poly(methylene oxide) creates localized vibrational modes, the anharmonic forces in poly(methylene oxide) (which corresponds to the third-order or even higher-order terms in the force field expression) induces frequent energy exchanges between the localized modes and leads to an increase in β value.³¹ The fitting of thermal conductivity κ with chain length L using the formula $\kappa \sim L^\beta$ is merely used to compare the diffusive phonon transport and ballistic phonon transport in polymer chains. The β value indicates the relatively dominant phonon transport mechanism. The β value does decrease from a short chain to a longer chain. However, this formula is by no way rigorously quantitative

and not suitable for extrapolating to chains with infinite length. Figure 2(d) shows that the fitting value of β is 0.411 from 5 to 1000 nm and the value is 0.438 from 5 to 230 nm. Likely, the β value would decrease gradually with even longer chain length (much larger than the phonon mean free path) due to more intrinsic phonon scattering.

IV. CONCLUSIONS

Atomistic simulation studies were conducted for analyzing phonon transport mechanisms in single extended polymer chains of various polymers as a function of polymer chain length. It is found that the thermal conductivity of single extended polymer chains can be 1–2 orders of magnitude higher than their bulk counterparts. Moreover, the thermal conductivity of single extended polymer chains is a strong function of monomer type. For example, the thermal conductivity of the extended polymer chains with aromatic backbone can be up to 5 times as that of a polyethylene chain, while the thermal conductivity of the extended polymer chains with bond strength or mass disorder can be only 1/25 as that of a polyethylene chain. Phonon-boundary scattering dominates the phonon scattering mechanisms in a short polymer chain (e.g., number of segments $N < 50$ in the polyethylene chain), whereas intrinsic phonon scattering dominates in a long polymer chain (e.g., number of segments $N > 200$ in the polyethylene chain). Intrinsic phonon scattering has a dominant effect in phonon transport if the polymer chain has “disorder” compared to the aliphatic/aromatic pristine chain. Moreover, the competition between ballistic phonon transport and diffusive phonon transport in the chain leads to a diverging length-dependent thermal conductivity of a single extended polymer chain.

ACKNOWLEDGMENTS

The authors would like to thank Dr. Xiaobo Li, Mr. Xiaokun Gu, and Mr. Mohamed Alhashme for valuable discussions. This work is supported by NSF CAREER award (Grant No. 0846561) and AFOSR STTR Grant (No. FA9550-112-C-0061).

*ronggui.yang@colorado.edu

¹D. J. David, *Relating Materials Properties to Structure: Handbook and Software for Polymer Calculations and Materials Properties* (Technomic, PA, 1999).

²C. L. Choy, *Polymer* **18**, 984 (1977).

³T. Shimoda, M. Kimura, S. Miyashita, R. H. Friend, J. H. Burroughes, and C. R. Towns, *SID Int. Symp. Digest Tech. Papers* **30**, 372 (1999).

⁴W. U. Huynh, J. J. Dittmer, and A. P. Alivisatos, *Science* **295**, 2425 (2002).

⁵A. Henry and G. Chen, *Phys. Rev. Lett.* **101**, 235502 (2008).

⁶S. Shen, A. Henry, J. Tong, R. Zheng, and G. Chen, *Nat. Nano.* **5**, 251 (2010).

⁷X. Huang, G. Liu, and X. Wang, *Adv. Mater.* **24**, 1482 (2012).

⁸T. Luo, K. Esfarjani, J. Shiomi, A. Henry, and G. Chen, *J. Appl. Phys.* **109**, 074321 (2011).

⁹K. Kurabayashi, *Int. J. Thermophys.* **22**, 277 (2001).

¹⁰S. M. George, B. Yoon, and A. A. Dameron, *Acc. Chem. Res.* **42**, 498 (2009).

¹¹H. Sun, S. J. Mumby, J. R. Maple, and A. T. Hagler, *J. Am. Chem. Soc.* **116**, 2978 (1994).

¹²Accelrys Inc., San Diego, 2003.

¹³S. Plimpton, *J. Comput. Phys.* **117**, 1 (1995).

¹⁴C. Oligschleger and J. C. Schon, *Phys. Rev. B* **59**, 4125 (1999).

¹⁵P. K. Schelling, S. R. Phillpot, and P. Keblinski, *Phys. Rev. B* **65**, 144306 (2002).

¹⁶P. K. Schelling, S. R. Phillpot, and P. Keblinski, *J. Appl. Phys.* **95**, 6082 (2004).

- ¹⁷G. J. Martyna, M. L. Klein, and M. Tuckerman, *J. Chem. Phys.* **97**, 2635 (1992).
- ¹⁸S. Berber, Y.-K. Kwon, and D. Tomanek, *Phys. Rev. Lett.* **84**, 4613 (2000).
- ¹⁹D. Brown and J. H. R. Clarke, *Macromolecules* **24**, 2075 (1991).
- ²⁰S. Lepri, R. Livi, and A. Politi, *Phys. Rep.* **377**, 1 (2003).
- ²¹J. Liu and R. Yang, *Phys. Rev. B* **81**, 174122 (2010).
- ²²G. Chen, *Nanoscale Energy Transport and Conversion: A Parallel Treatment of Electrons, Molecules, Phonons, and Photons* (Oxford University Press, Oxford, 2005).
- ²³D. M. Heyes, *Chem. Phys.* **82**, 285 (1983).
- ²⁴J. D. Gale and A. L. Rohl, *Mol. Simulat.* **29**, 291 (2003).
- ²⁵Z. Rieder, J. L. Lebowitz, and E. Lieb, *J. Math. Phys.* **8**, 1073 (1967).
- ²⁶A. Casher and J. L. Lebowitz, *J. Math. Phys.* **12**, 1701 (1971).
- ²⁷N. Yang, G. Zhang, and B. Li, *Nano Today* **5**, 85 (2010).
- ²⁸N. Mingo and D. A. Broido, *Nano Lett.* **5**, 1221 (2005).
- ²⁹B. Li and J. Wang, *Phys. Rev. Lett.* **91**, 044301 (2003).
- ³⁰A. Ward and D. A. Broido, *Phys. Rev. B* **81**, 085205 (2010).
- ³¹D. N. Payton, III, M. Rich, and W. M. Visscher, *Phys. Rev.* **160**, 706 (1967).